Division of Drugs[1], National Institute of Health Sciences; Tokyo Metropolitan Industrial Technology Research Institute[2], Tokyo, Japan

NIR spectroscopic investigation of two fluoroquinolones, levofloxacin and ofloxacin, and their tablets for qualitative identification of commercial products on the market

T. Sakamoto[1], Y. Fujimaki[2], Y. Hiyama[1]

Received April 4, 2008, accepted April 24, 2008

T. Sakamoto, Ph.D., National Institute of Health Sciences, Tokyo 158-8501, Japan
tsakamot@nihs.go.jp

Pharmazie 63: 628–632 (2008) *doi: 10.1691/ph.2008.8107*

A rapid and nondestructive identification method for ofloxacin (OFLX) and levofloxacin (LVFX) utilizing diffusion reflectance near-infrared (NIR) spectroscopy was developed. An obvious difference in spectral patterns between LVFX that is used for commercial tablets and LVFX HCl that can be purchased as a reagent at a low price was also observed. These quinolones are especially important for use as drugs against bio-terrorism because of their effectiveness against anthrax infection. Therefore, the possibility of a distribution of counterfeit drugs containing LVFX HCl on the market would be expected. NIR spectroscopic analysis would be applicable to on-site quality analysis that can be carried out easily and nondestructively.

1. Introduction

Quinolone synthetic antibiotics have been used widely for various bacterial infectious diseases because they have a wide antibacterial spectrum. Up to now, more than 20 quinolones have been developed and approved all over the world. Ofloxacin ((3*RS*)-9-Fluoro-2,3-dihydro-3-methyl-10-(4-methylpiperazin-1-yl)-7-oxo-7*H*-pyrido[1,2,3-*de*]-1,4-benzoxazine-6-carboxylic acid, OFLX) and levofloxacin ((−)-(*S*)-9-fluoro-2,3-dihydro-3-methyl-10-(4-methyl-1-piperazinyl-7-oxo-7*H*-pyrido[1,2,3-*de*][1,4]benzoxazine-6-carboxylic acid hemihydrate, LVFX) were developed in 1980s. OFLX is a racemate, and LVFX is an L-enantiomer. LVFX has a wider antibacterial spectrum than OFLX, and, in addition to ciprofloxacin hydrochloride, it can also be used for treatment of anthrax infection.

Although several analytical methods of quinolone antibacterials have been reported (Koechlin et al. 1989; Tyczkowska et al. 1989; Bauer et al. 1990; Nangia et al. 1990; Barbato et al. 1994; Zhai et al. 1995; Barbosa et al. 1998; Wright et al. 1998), most of these utilize destructive analytical methodologies such as chromatography. In order to separate enantiomers such as LVFX (L-enantiomer) and OFLX (racemate) during a screening analysis, conventional chromatographic conditions with reverse-phase silica gel solid phase will be used first, followed by HPLC with columns for optically active substances.

Recently, near-infrared (NIR) spectroscopy has been widely applied in the pharmaceutical industrial field as an analytical tool for Process Analytical Technology (PAT) because it can provide nondestructive analyses of spectral properties of both liquid and solid samples (Scafi et al. 2001; Fountain et al. 2003; Li et al. 2003; Sandler et al. 2005; El-Hagrasy et al. 2006; El-Hagrasy 2006; Medendorp et al. 2006). An NIR spectrum contains information on chemical functional groups and physical conditions such as particle size. Also, it is generally sensitive to chemical and physical environment changes. Accordingly, it may provide distinguished spectral information regarding pharmaceutical ingredients and products. As a result, NIR will likely show unique spectral properties based on the pharmaceuticals specific to the manufacturing process and the process controls employed. It can therefore be employed for the identification of pharmaceutical products on the market, e.g. counterfeit drugs, and for confirmation of

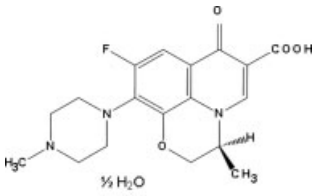

LVFX

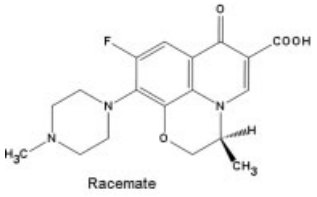

Racemate

OFLX

product quality (Jernigan et al. 2001; Westenberger et al. 2005). Determination of enantiomers and racemate using NIR spectroscopy has been reported (Luner et al. 2005). In that paper, it was speculated that the difference in the arrangement of molecules between enantiomers and racemate contributes to the different crystal structures.

In the present study, we have developed a nondestructive identification method for LVFX tablets and OFLX tablets using diffusion reflectance NIR spectrometry, and the applicability of this analytical method for use with tablets on the market was also examined.

2. Investigations and results

2.1. Diffusion reflectance NIR spectrum of LVFX and OFLX

2.1.1. First overtone range of C−H of NIR spectra

The raw NIR spectra and observed wave numbers that characterize the chemical structure of these substances are shown in Fig. 1 and the Table, respectively. In the range of wave numbers from 9500 cm^{-1} to 4000 cm^{-1}, vibration bands of C−Hs were expected to be detectable from the chemical structures of both substances. The whole spectrum was classified in the wave number ranges that were the first overtone of C−H (A: 6200 cm^{-1} to 5600 cm^{-1}, aromatic and alkyl) and the second overtone of C−H (B and C: 9500 cm^{-1} to 6500 cm^{-1}). Figure 2 shows the first overtone range of raw NIR spectra of LVFX and OFLX. These spectra were normalized to compare with same relative intensity between these substances. The numbers labeled in the spectra in Fig. 3 correspond to those shown in the Table. The absorbance of OFLX was observed to be lower than that of LVFX through the entire measured wave number range. Moreover, the wave numbers of the detected peaks did not correspond between the two substances, and each substance showed its characteristic waveform. In the range from 6000 cm^{-1} to 5900 cm^{-1}, which was the range of the first overtone of C−H (aromatic), five peaks in the vicinity of peak number 6 through 10 were observed from both second derivative wave forms, but no exact corresponding peaks between the two substances were observed. In particular, the absorbance intensities of the two peaks at 5941 cm^{-1} and 5925 cm^{-1} of LVFX were significantly larger than that of OFLX. This phenomenon was thought to be due to the one direction of molecule arrangement of LVFX crystalline powder as the L enantiomer providing a larger vibration intensity of C−H than that of OFLX, as a racemate having two kinds of molecular arrangements.

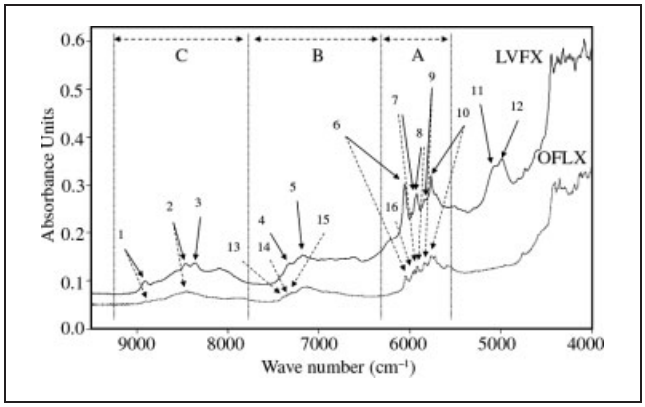

Fig. 1: Typical NIR spectra of LVFX standard (shown as the solid line) and OFLX standard (shown as the broken line). Different waveforms between LVFX and OFLX were observed. The numbers in the figure correspond to those in the Table

Table: Unique wave numbers of LVFX and OFLX (The wave number with underline corresponds to the wave numbers of OFLX)

9000 — 8000 — 7000 — 6000 — 5000 — 4000 (cm^{-1})

2nd Overtone region — Combinations

1st Overtone region

3rd Overtone region

CH_3 — C−H Comb. — C−H, Ar−C−H — O−H Comb

1 8909 cm^{-1}: CH_3 2nd overtone*

8893 cm^{-1}:

2 8465 cm^{-1}: CH_3, Str., 2nd overtone

8457 cm^{-1}:

3 8360 cm^{-1}: CH_2, Str., 2nd overtone

19 8090 cm^{-1}: CH, Str., 2nd overtone*

4 7324 cm^{-1}: CH_3, Comb., 2 × CH str. + CH bend

5 7189 cm^{-1}: CH_2, Comb., 2 × CH str. + CH def

6 6058 cm^{-1}: CH, Comb., 1st overtone*

6051 cm^{-1}:

13 7390 cm^{-1}: CH_3, Comb., 2 × CH stret, + CH bend.*

7 5941 cm^{-1}: CH (aromatic), 1st overtone

5950 cm^{-1}:

14 7343 cm^{-1}: CH_3, Comb., 2 × CH stret, + CH bend.*

8 5925 cm^{-1}: CH (aromatic), 1st overtone

5918 cm^{-1}:

15 7306 cm^{-1}: CH_3, Comb., 2 × CH stret, + CH bend.*

9 5837 cm^{-1}: CH_3, 1st overtone of asym. stret.

5840 cm^{-1}:

10 5768 cm^{-1}: CH_3, 1st overtone of antisym., stret.

5768 cm^{-1}:

16 5967 cm^{-1}: CH, 1st overtone*

11 5071 cm^{-1}: O−H comb.*

12 4991 cm^{-1}: O−H comb.*

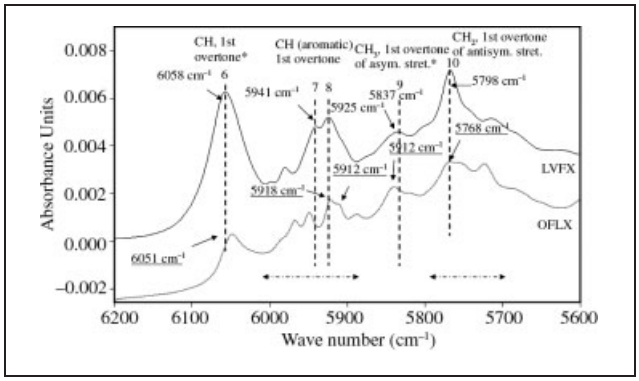

Fig. 2: The vector-normalized NIR spectra of the C−H first overtone region of LVFX (shown as the solid line) and OFLX (shown as the broken line). The wave numbers of the detected peaks do not correspond between the two compounds, and each compound shows the characteristic spectrum

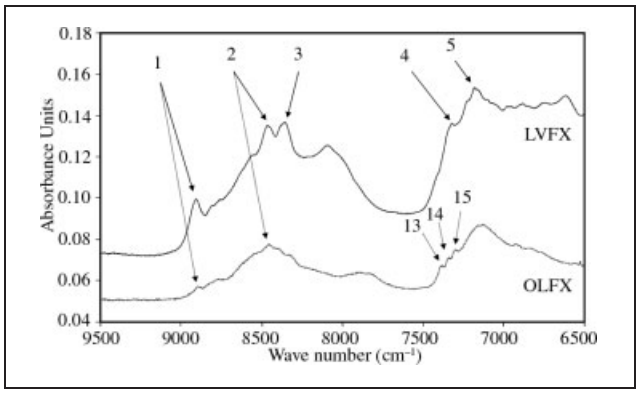

Fig. 3: The NIR spectra of C−H second overtone and the first overtone of the C−H combination region of LVFX (the solid line) and OFLX (the broken line). Different waveforms between the two substances were also observed in this range

2.1.2. Second overtone of C−H and the combination range of C−H of NIR spectra

The raw NIR spectra of ranges of second overtones and the combination of C−H in both quinolones are shown in Fig. 3. The spectra of both substances were different. The peak at 8908 cm^{-1} (Peak No. 1) that was the second overtone of CH_3, the peaks at 8465 cm^{-1} (Peak No. 2) and 8360 cm^{-1} (Peak No. 3) that were the second overtone of the CH_3 and CH_2 stretching vibrations, and the peaks at 7324 cm^{-1} (Peak No. 4) and 7189 cm^{-1} (Peak No. 5) that were the combination of CH_3 and CH_2 were observed on LVFX. In the case of OFLX, the peaks that were the second overtone of CH_3 (8893 cm^{-1}, Peak No. 1), the second overtone of CH_3 stretching (8457 cm^{-1}, Peak No. 2), and three peaks that were the combinations of C−H (from 7390 cm^{-1} to 7306 cm^{-1}) were observed.

2.2. Influence of HCl salt on the diffusion reflectance NIR spectrum of LVFX

Figure 4 shows the raw NIR spectra in the range of the first overtone of C−H of both substances. The absorption intensity of the waveform of LVFX HCl was weaker than that of LVFX. In the raw spectrum of LVFX HCl, nine peaks were observed in the wave-number range from 6060 cm^{-1} to 5830 cm^{-1}, while seven peaks were detected in the same wave numbers range of LVFX. The peak at 5998 cm^{-1} was detected from both substances. It was presumed that this peak was not affected by the intermolecular energy of HCl.

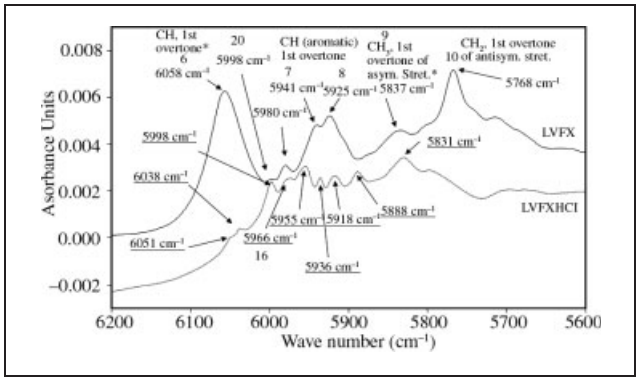

Fig. 4: The vector-normalized NIR spectra of the C−H (aromatic) first overtone region of LVFX (shown as the solid line) and LVFX HCl (shown as the broken line). LVFX HCl gave its own spectrum compared with LVFX. The wave number with an underline refers to the peaks obtained from LVFX HCl

This observation suggests that this absorption corresponds to the first overtone of C−H that was located at the most unaffected position was distant from HCl.

2.3. NIR analysis of commercial LVFX tablets

Figure 5 shows the NIR spectrum of the Cravit Tablet® using the optical fiber probe. Several characteristic peaks corresponding with the peaks of the LVFX standard were observed. In addition, the powdered tablets were subject to the NIR measurements in order to obtain NIR spectral information on all the ingredients in the tablet. The five peaks (Nos. 1, 2, 3, 6, 10) were observed in the three NIR spectra. The second derivative spectra in the range of the first overtone of C−H in the three spectra of LVFX, the Cravit Tablet®, and the powdered tablet are shown in Fig. 6. The six characteristic peaks at 6058 cm^{-1} (Peak No. 6), 5998 cm^{-1} (Peak No. 20), 5981 cm^{-1} (Peak No. 21), 5941 cm^{-1} (Peak No. 7), 5925 cm^{-1} (Peak No. 8), and 5768 cm^{-1} (Peak No. 10) were observed in this range. The peaks at 6058 cm^{-1} (No. 6, first overtone of C−H) and 5768 cm^{-1} (No. 10, first overtone of CH_2 anti-symmetric stretching) were observed as overlapping with the other peak of the ingredient. However, these two peaks were not observed in the second derivative NIR spectrum obtained from powdered tablets. Although further studies will be needed, it appears that the average spectrum of all ingredients, including the coating film that was included in the powdered tablets, was obtained. The spectrum ob-

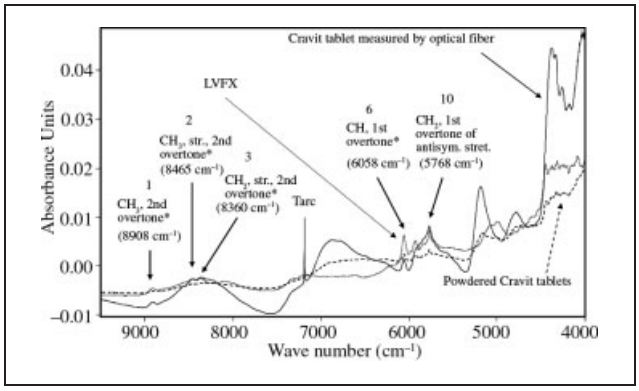

Fig. 5: Typical NIR spectra of LVFX (shown as the solid line), the Cravit tablet (shown as the broken line, obtained by using an optical fiber probe), and powdered Cravit tablets (shown as the large broken line). Several peaks correspond among the three spectra

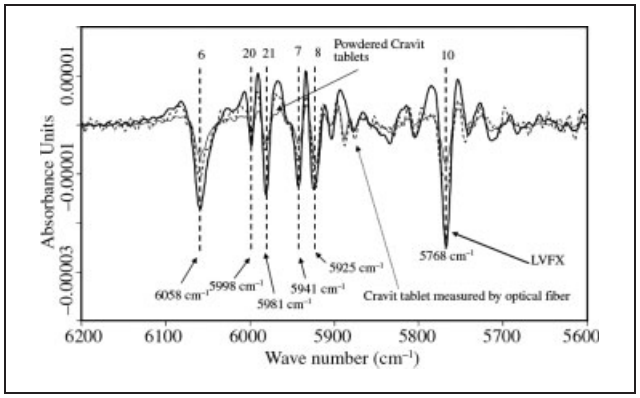

Fig. 6: The vector-normalized and second derivative NIR spectra of the C−H first overtone region of LVFX (the thick solid line), the Cravit tablet (the broken line), and powdered Cravit tablets (the thin solid line). Several peaks have a characteristic shape that would be caused by overlapping with peaks of medical additives.

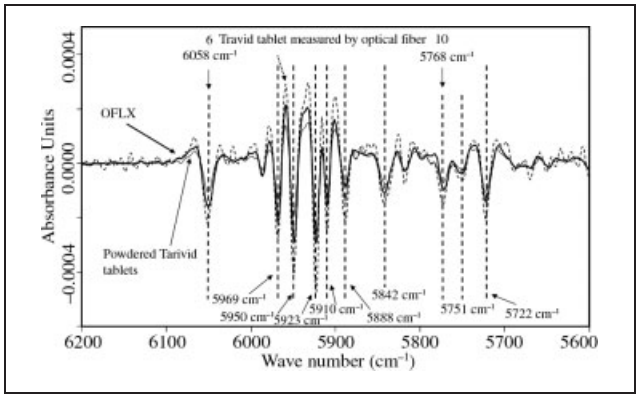

Fig. 8: C−H first overtone region of second derivative NIR spectra of OFLX (shown as the thick solid line), the Tarivit tablet (shown as the broken line), and powdered Tarivit tablets (shown as the thin solid line). A total of ten characteristic peaks were corresponding among the three spectra.

tained from the powdered tablets would affect the shape of the peak compared with that of the intact tablet.

2.4. Discrimination of LVFX in a tablet and in LVFX HCl

Discrimination between LVFX in the LVFX tablet and LVFX HCl was examined. The second derivative spectra of the first overtone of C−H that was obtained from the Cravit Tablet® by using an optical fiber probe and from LVFX HCl in a glass vial are shown in Fig. 7. One peak at 5998 cm^{-1} (Peak No. 20) was observed that corresponded to the observed 6 peaks that are shown in Fig. 6. In other words, 5 peaks numbered 6, 7, 8, 10, and 21 obtained from the LVFX standard were not matched with peaks obtained from LVFX HCl. This result suggests that NIR spectroscopy is applicable with high specificity to identify counterfeit drugs on the market containing LVFX HCl compared with legal products containing LVFX.

2.5. NIR analysis of intact OFLX tablets

The typical second derivative NIR spectra in the range of the first overtone of C−H were obtained from the Tarivid Tablet® containing OFLX are shown in Fig. 8. In the three spectra obtained from OFLX, the Tarivid Tablet® (using optical fiber probe), and finely powdered Tarivid Tablet®, a total of 10 characteristic peaks were observed. These results suggest that diffusion reflectance NIR spectroscopy is applicable to nondestructive detection of OFLX in the Tarivit Tablet® on the market.

In the second derivative spectra range in these products, characteristic peaks of each active drug in tablet were observed. It was also suggested that this spectroscopic method would allow for easy identification of LVFX and OFLX in the tablet by analysis of NIR spectra of the first overtone range of C−H.

In conclusion nondestructive discrimination between LVFX and OFLX was achieved by using diffusion reflectance NIR spectrometry. This result suggests that NIR spectroscopy is applicable to rapid and nondestructive identification of intact tablets containing racemate and enantiomers.

Moreover, NIR spectroscopy would be applicable as an analytical tool for not only a control of enantiomers in the pharmaceutical development stage and manufacturing process but also for on-site quality analysis of pharmaceutical products on the market.

Spectral information obtained from pharmaceutical products that have been controlled by appropriate GMP activities will provide a certification that is like a fingerprinting. Although it is known that a spectrum obtained by diffusion reflectance NIR measurements would be affected by various deviation factors (Ozaki et al. 1998; Yoon et al. 1998; O'Neil et al. 2003; Sakamoto et al. 2007), use of these spectra has the potential to aid in detection of different kinds of products with different manufacturing processes. The practical use of fingerprint-like spectral analysis of commercial products utilizing NIR spectrometry for rapid and nondestructive on-site quality analysis is therefore expected.

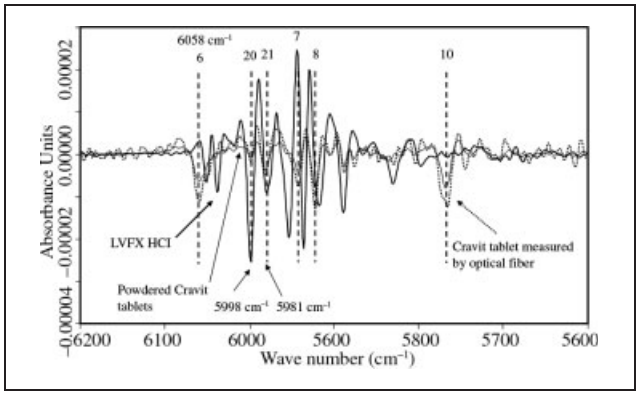

Fig. 7: The vector-normalized and second derivative NIR spectra of the C−H first overtone region of LVFX HCl (shown as the thick solid line), the Cravit tablet (shown as the broken line), and powdered Cravit tablets (shown as the thin solid line)

3. Experimental

3.1. NIR instrument

Diffusion reflectance NIR measurements were performed using an MPA FT-NIR (Bruker Optics K.K., Ettlingen, Germany).

3.2. Materials

Reagents of LVFX, LVFX hydrochloride, and OFLX were purchased from Wako Chemical Inc (Tokyo, Japan) and were used without further purification. Cravit Tablets® 100 mg (Daiichi Pharmaceutical Co Ltd, Tokyo, Japan) and Tarivid Tablets® were purchased from a commercial source.

3.3. Sample measurements and measurement conditions

LVFX, LVFX HCl, and OFLX reagents were put into glass vials that were made for MPA measurements (Bruker Optics Inc., Ettlingen, Germany). Each vial was then placed on a radiation port for the diffusion reflectance

NIR measurement as a standard substance. A tablet holder from Bruker Optics Inc. was used to measure the tablets. The tablet holder with a tablet was placed on the radiation port, which was then measured by a transmittance or reflectance NIR spectroscopic mode. To make powdered tablets, seven tablets were put in the mortar and were crushed by grinding. Fragments of the film coating were also ground down to similar size as the other ingredients. Then, whole powder was placed into a glass vial and measured in the same manner as the standard substances.

When the optical fiber probe was used for measurements, a tablet was fixed at the top of the probe with adhesive tape. All measurements were performed under the following conditions. The measurement range, scan wave number interval, resolution, and numbers of integration steps were 12000 cm^{-1} to 4000 cm^{-1}, 2 cm^{-1}, 4 cm^{-1}, and 64, respectively.

References

Barbato F, Morrica P, Seccia S, Ventriglia M (1994) High performance liquid chromatographic analysis of quinolone antibacterial agents. Farmaco 49: 407–410.

Barbosa J, Bergés R, Sanz-Nebot V (1998) Retention behaviour of quinolone derivatives in high-performance liquid chromatography, Effect of pH and evaluation of ionization constants. J Chromatgr A 823: 411–422.

Bauer JF, Elrod Jr. L, Fornnario JR, Heathcote DE, Krogh SK, Linton CL, Norris BJ, Quick JE (1990) Determination of temafloxacin, sarafloxacin, and difloxacin in bulk drug and dosage forms by high-performance liquid chromatography. Pharm Res 7: 1177–1180.

El-Hagrasy AS, D'Amico F, Drennen JK (2006) A process analytical technology approach to near-infrared process control of pharmaceutical powder blending. Part I: D-optimal design for characterization of powder mixing and preliminary spectral data evaluation. J Pharm Sci 95: 392–406.

El-Hagrasy AS, Drennen JK (2006) A process analytical technology approach to near-infrared process control of pharmaceutical powder blending. Part III: Quantitative near-infrared calibration for prediction of blend homogeneity and characterization of powder mixing kinetics. J Pharm Sci 95: 422–434.

Fountain W, Dumstorf K, Lowell AE, Lodder RA, Mumper RJ (2003) Near-infrared spectroscopy for the determination of testosterone in thin-film composites. J Pharm Biomed Anal 33: 181–189.

Jernigan JA, Stephens DS, Ashfold DA, Omenaca C, Topiel MS, Galbraith M, Tapper M, Fisk TL, Zaki S, Popovic T, Meyer RF, Quinn CP, Harper SA, Fridkin SK, Sejvar JJ, Shepard CW, McConnel M, Guarner J, Shieh Wun-Ju, Malecki JM, Gerberging JL, Hughes JM, Perkins BA, member of the Anthrax Bioterrorism Investigation Team (2001) Bioterrorism-related inhalational anthrax: The first 10 cases reported in United States. Emerging Infectious Diseases CDC, **7**: No. 6.

Koechlin C, Jehl F, Linger L, Monteil H (1989) High-performance liquid chromatography for the determination of three new fluoroquinolones, fleroxacin, temafloxacin and A-64730, in biological fluids. J Chromatogr Biom Appl 491: 379–387.

Li T, Donner AD, Choi CY, Frunzi GP, Morris KR (2003) A statistic support for using spectroscopic methods to validate the content uniformity of solid dosage forms. J Pharm Sci 92: 1526–1530.

Luner PE, Patel AD (2005) Quantifying crystal form content in physical mixture of (±)-tartaric acid and (+)-tartaric acid using near infrared reflectance Spectroscopy. AAPS PharmSciTech 6: E245–E252.

Medendorp J, Buice Jr. RG, Lodder RA (2006) Acoustic-resonance spectrometry as a process analytical technology for the quantification of active pharmaceutical ingredient in semi-solids. AAPS PharmSciTech 7: E1–E8.

Nangia A, Lam F, Cheung-Tak H (1990) Reversed-phase ion-pair high-performance liquid chromatographic determination of fluoroquinolones in human plasma. J Pharm Sci 79: 988–991.

O'Neil AJ, Jee RD, Moffat AC (2003) Measurement of the percentage volume particle size distribution of powdered microcrystalline cellulose using reflectance near-infrared spectroscopy. Analyst 128: 1326–1330.

Ozaki K (ed.) (1998) "Kinsekigai bunkouho (Near Infrared spectroscopy): Sakurai K. Near infrared spectrometry and experimental method. (IPC, Japan), pp. 71–93. (in Japanese)

Sakamoto T, Fujimaki Y, Hiyama Y (2007) Studies on the influence of uniformity of particle size of powder, tapping and sample replacement for diffusion reflectance quantitative NIR spectrometric analysis. Pharmazie 62: 841–846.

Sandler N, Rantanen J, Heinamaki J, Romer M, Marvola M, Yliruusi J (2005) Pellet manufacturing by extrusion-spheronization using process analytical technology. AAPS PharmSciTech 6: E174–E183.

Scafi SH, Pasquini C (2001) Identification of counterfeit drugs using near-infrared spectroscopy. Analyst 126: 2218–2224.

Tyczkowska K, Hedeen KM, Aucoin DP, Aronson AL (1989) High-performance liquid chromatographic method for the simultaneous determination of enrofloxacin and its primary metabolite ciprofloxacin in canine serum and prostatic tissue. J Chromatgr Biom Appl 493: 337–346.

Westenberger BJ, Ellison CD, Fussner AS, Jenney S, Kolinski RE, Lipe TG, Lyon RC, Moore TW, Revelle LK, Smith AP, Spencer JA, Story KD, Toler DY, Wokovich AM, Buhse LF (2005) Quality assessment of internet pharmaceutical products using traditional and non-traditional analytical techniques. Int J Pharm 306: 56–70.

Wright DH, Herman VK, Konstantinides FN, Rotschafer JC (1998) Determination of quinolone antibiotics in growth media by reversed-phase high-performance liquid chromatography. J Chromatogr B 709: 97–104.

Yoon WL, Jee RD, Moffat AC (1998) Optimization of sample presentation for the near-infrared spectra of pharmaceutical excipients. Analyst 123: 1029–1034.

Zhai S, Korrapati MR, Wei X, Muppalla S, Vestal RE (1995) Simultaneous determination of theophylline, enoxacin and ciprofloxacin in human plasma and saliva by high-performance liquid chromatography. J Chromatogr B 669: 372–376.